Observations of indirect exciton trapping in one- and two-dimensional magnetic lattices

A. Abdelrahman and Byoung S. Ham

Center for Photon Information Processing, School of Electrical Engineering, Inha University, Incheon 402-751, South Korea

(Received 23 February 2012; revised manuscript received 29 May 2012; published 23 August 2012)

A simple method to create and control magnetic potentials on coupled quantum wells is demonstrated for indirect exciton magnetic confinement. Localized inhomogeneous magnetic potentials with periodically distributed local minima and maxima, known as magnetic lattices, are projected into the plane of the coupled quantum wells and used for spatially distributed two-dimensional indirect exciton trapping, in which case localized indirect excitons are observed. The indirect exciton trapping mechanism is examined by controlling the external magnetic field bias, resulting in a shift of the localized excitonic lattice.

DOI: 10.1103/PhysRevB.86.085445 PACS number(s): 71.35.Ji, 52.55.Jd, 52.55.Lf

In quantum heterostructures such as coupled quantum wells (CQWs), the presence of an artificially exerted confining potential quantizes the motion of quantum particles in discrete levels determined by the confining fields. Such confinement plays an important role for the control of quantum particles and opens a new direction for simulation of condensed-matter systems and to process quantum information in semiconductors. Interesting results have been recently reported for indirect exciton trapping in CQWs using periodic electrical potentials.[1–4] In particular, trapping of indirect excitons has been demonstrated by an electric potential for a single electrostatic trap,[5–8] a one-dimensional electrostatic lattice,[3] and two-dimensional electrostatic lattices.[9,10] Meanwhile, special attention has been paid to magnetic field confinement as an alternative stable trapping mechanism for the indirect excitons,[11–14] where stable magnetic traps can be produced by using permanent magnetic materials.[15] Integration of magnetic materials with a quantum well system has been proposed theoretically[11,16] and demonstrated experimentally.[14,17]

In this article we present a clear signature of stable magnetic confinement of indirect excitons in both one- and two-dimensional magnetic lattices within a system of CQWs. The observed trapped indirect excitons are periodically distributed and controlled by shifting the trapping magnetic field local minima and maxima using a modulating external magnetic bias field. The confinement stability of the inhomogeneous magnetic field is due to the use of permanently magnetized material to produce the trapping fields. The magnetic field's local minima and maxima projected onto CQWs as shown in Fig. 1 are the origin of the magnetic confinement in a similar way to the magnetic trapping of ultracold atoms.[15,18] The magnetic field local minima $B_{\min}$ are realized by fabricating specific patterns in a permanently magnetized thin film of thickness τ, in which case the patterns extend through the thin film down to the surface of the underlying CQW layers. The presence of the patterns results in local field minima and maxima that appear at effective distances $d_{\min}$ above the top and the bottom of the magnetized thin film, as shown in Fig. 1(c). The effective distance is defined as $d_{\min} \approx \frac{\alpha}{\pi} \ln(B_{\text{int}})$ where α represents both the length (α_h) of each pattern and the separation (α_s) between patterns, $B_{\text{int}} = B_0\{1 - \exp[-(\pi/\alpha)\tau]\}$ with $B_0 = \mu_0 M_z/\pi$ and M_z the magnetization along the z axis.[15] Thus, the $d_{\min}$ is determined by the pattern parameter α (α_h and α_s) and τ. Depending on the shape and the number of the patterns the magnetic field local minima can be periodically distributed as simulated for the case of two-dimensional magnetic lattices in Fig. 1(d).

The center of each of the local field minima (i.e., the magnetic bottom of each single lattice site with $B = B_{\min}$) is surrounded by relatively high fields known as magnetic barriers $\Delta B(k)$ which define the space of the confinement and its depth, $\Delta B(k) = |B_{\max}(k)| - |B_{\min}(k)|$. The curvature along the confining directions determines the trapping frequency ω_k which depends on the Zeeman levels of the trapped particles. For the case of a harmonic potential (i.e., individual single site) the trapping frequency is given by $\omega_{k\equiv x,y} = \frac{\beta}{2\pi}\sqrt{\mu_B g_F m_F \frac{\partial^2 B}{\partial k^2}}$ and $\omega_z = \sqrt{\omega_x^2 + \omega_y^2}$, where g_F is the Landé g factor, μ_B is the Bohr magneton, and m_F is the magnetic quantum number of the hyperfine states.[15]

Here we consider the ground state of the free indirect excitons to be optically active, resulting in recombination in a narrow radiative zone with a momentum close to zero.[19] As schematically represented in the inset (1) of Fig. 1(b), the indirect excitons are spatially trapped in their ground states at the bottom of each single trap. The bottom of the trap is a space point where the trapping magnetic field is at its minimum value and points perpendicularly to the x-y plane of the integrated magnetic CQWs; the total field at this location is denoted by $B_\perp$. Note that the quantum well growth direction is along the z axis. Around each magnetic local minimum (lattice site), the magnetic field is relatively higher with a direction parallel, $B_\parallel$, to the x-y plane of the CQWs. At $B_\parallel$ locations the indirect exciton's momentum increases at the cost of its energy. The difference in the excitons' energies defines the trapping energy. The exciton energy is defined as $E_{\text{ext}}(P) = -E_B e^{-\sigma} I_0(-\sigma)$, where $I_0(-\sigma)$ is the modified Bessel function, E_B is the binding energy, $\sigma = (\frac{Pl_B}{2\hbar})^2$, and $l_B = \sqrt{\frac{\hbar c}{eB}}$ is the magnetic length. For indirect excitons at nearly zero momentum, the magnetic length l_B is comparable to the Bohr radius a_B where in the case of short magnetic length $l_B < a_B$, the spin part of the dominant indirect exciton wave function is deformed and also causes the Zeeman splitting. For a small separation ($\ll l_B$) between the electron (e) and hole (h) layers in CQWs subject to magnetic fields, the ground state of the system results from the e-h interaction, leading to a confined cloud of indirect excitons that is sufficiently extended in the confining space.[20] In the present experiments,

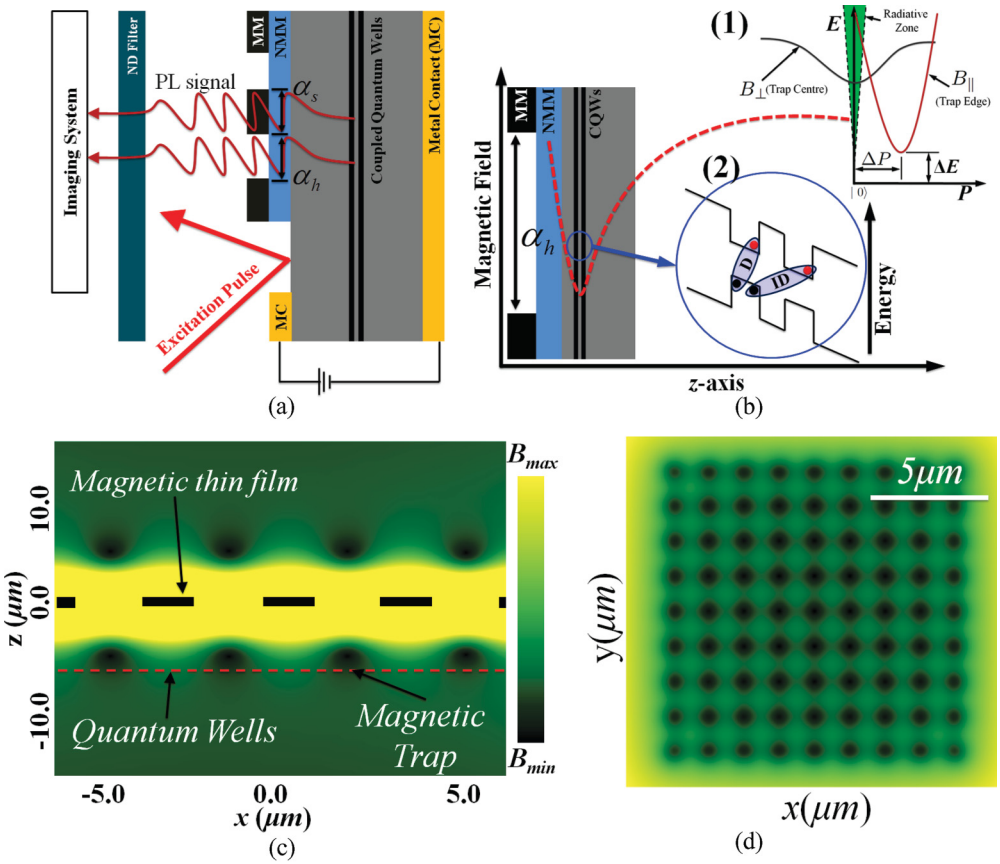

FIG. 1. (Color online) (a) Schematic diagram of the experimental setup showing the integrated magnetic coupled-quantum-well system. The excitation pulse is set at $\ll$1000 μm away from the magnetic structure. (b) The existence of the hole in the permanent magnetic material creates a confining magnetic field with its minima projected into the location of the double quantum wells in which case the dispersion surface of the indirect excitons behaves according to the direction of the confining field as depicted in the inset (1). (c),(d) The simulated magnetic field of a two-dimensional magnetic lattice with $\alpha_s = \alpha_h = 3.5$ μm and $\tau = 2$ μm.

we fabricated the quantum well width at less than l_B (less than the Bohr radius of excitons in GaAs $\approx$13.5 nm). Thus, the indirect excitons are seen to mainly interact with the trapping inhomogeneous magnetic fields.

The double-quantum-well system of Fig. 1(b) is grown by molecular beam epitaxy, where the sample consists of two 8 nm GaAs quantum wells separated by a 4 nm $Al_{0.33}Ga_{0.67}As$ barrier and surrounded by two 200 nm $Al_{0.33}Ga_{0.67}As$ highly conducting layers. The metal contacts monitor the electric field along the z direction for indirect exciton generation; Fig. 2 shows the gate voltage V_G dependence of the emitted photoluminescence spectrum, indicating the energy shift of the indirect excitons with respect to V_G.

Using an rf sputtering technique, a nonmagnetic material, gadolinium gallium garnet (GGG) $Gd_3Ga_5O_{12}$, of thickness $\approx$3 μm is deposited on top of the CQW system, where the thickness of the nonmagnetic spacer determines the effective distance $d_{\min}$ and allocates the magnetic field local minima and maxima within the quantum well layers. The permanent magnetic material $Bi_2Dy_1Fe_4Ga_1O_{12}$ is deposited with a thickness of $\approx$2 μm on top of the whole system (GGG + CQWs), as shown in Fig. 1(b).

We demonstrate magnetic trapping in two types of magnetic lattice: (i) for one-dimensional magnetic lattices with dimensions $\alpha_h = \alpha_s = 5$ μm as shown in Figs. 3(a) and 3(b), and with $\alpha_h = 10$ μm, $\alpha_s = 30$ μm as shown in Fig. 4(a); and (ii) for two-dimensional magnetic lattices with $\alpha_h = \alpha_s = 3.5$ μm as shown in Figs. 3(c) and 3(d). The $Bi_2Dy_1Fe_4Ga_1O_{12}$

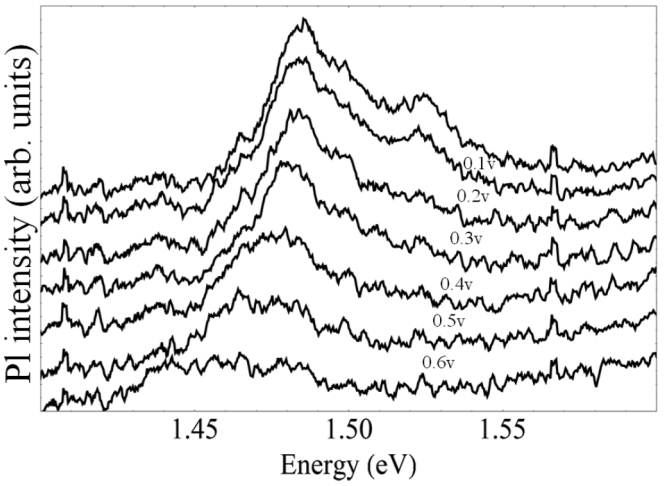

FIG. 2. Gate voltage V_G dependence of the emitted photoluminescence spectrum shows the shift in energy of the indirect excitons with respect to V_G using a pump laser with wavelength $\lambda = 632$ nm, excitation power $P_{\text{laser}} = 1$ mW, and $T = 25$ K.

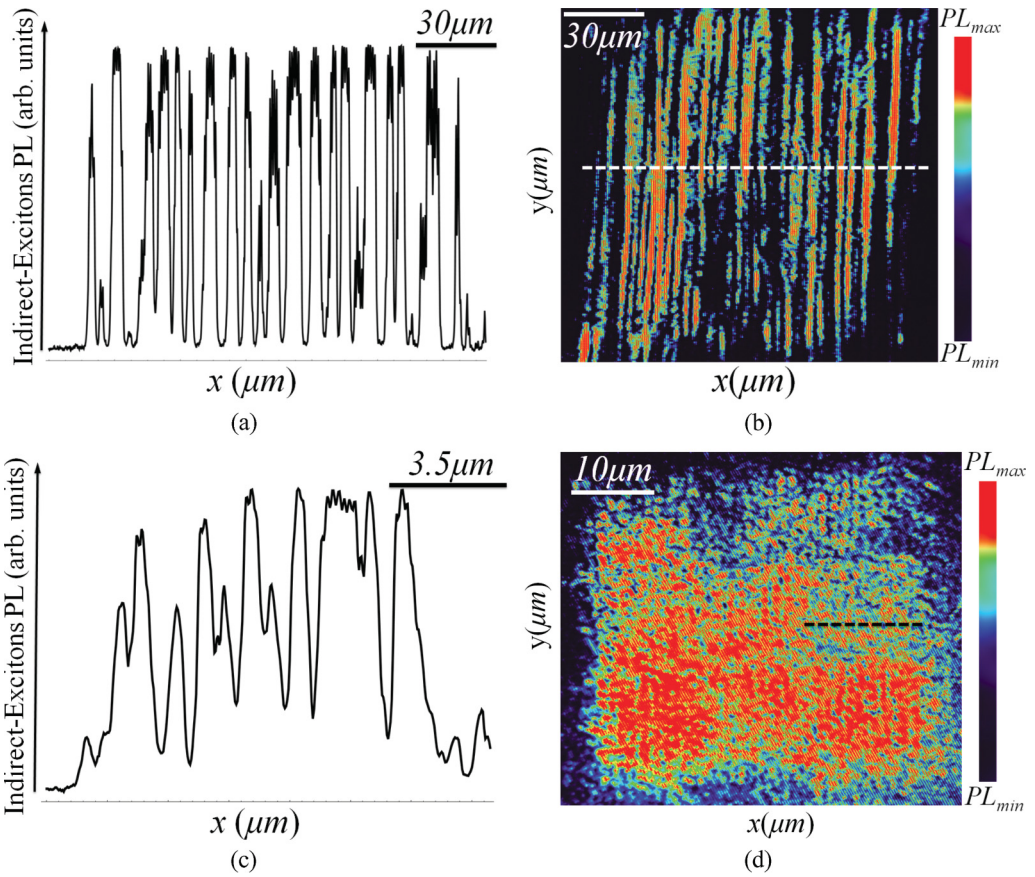

FIG. 3. (Color online) Experimental results for confined indirect excitons (a) and (b) for a one-dimensional magnetic lattice with dimension of $\alpha_s = \alpha_h = 5$ μm and (c) and (d) for a two-dimensional structure with experimental parameters $\alpha_s = \alpha_h = 3.5$ μm. In both structures the magnetic material thin-film thickness is $\tau = 2$ μm.

is transparent to light at wavelength $\lambda \geqslant 600$ nm,[21] where the indirect-exciton-generated photoluminescence is fully transmitted through the magnetic layer. The maximum intensity of the emitted indirect exciton photoluminescence at 13 K is found to be around 1.51 eV. The magnetic lattices for one- and two-dimensional structures are fabricated by using focused ion beam lithography, annealed at 876.15 K, etched, and externally magnetized with a magnetic field of 500 G before cooling to 13 K in a helium cryostat. The magnetizing magnetic field is applied perpendicular to the overall growth direction, resulting in magnetization of the $Bi_2Dy_1Fe_4Ga_1O_{12}$ layer along the z direction perpendicular to the surface of the

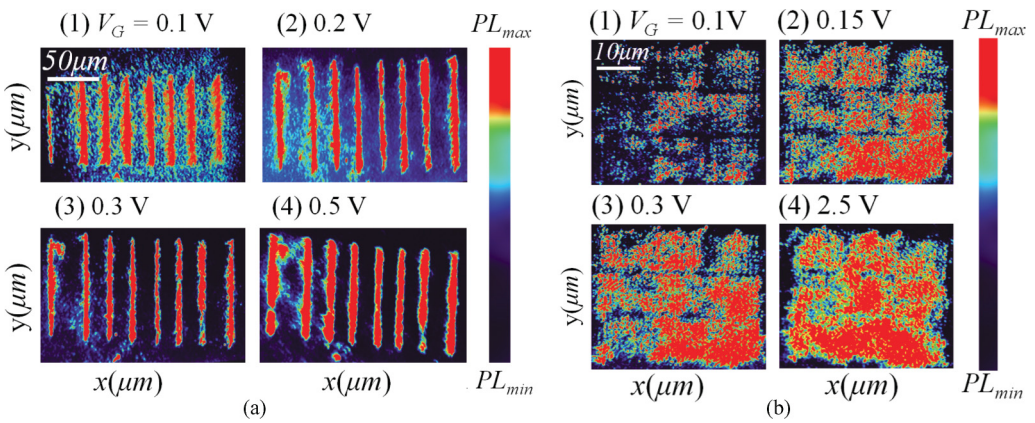

FIG. 4. (Color online) Effect of increasing the injection rate of the electrons and holes via the potential gate voltage V_G; enhanced photoluminescence is observed at each single magnetic trap. The experiments are conducted for (a) a one-dimensional magnetic lattice with dimensions of $\alpha_h = 10$ μm, $\alpha_s = 30$ μm, and $\tau = 2$ μm with excitation pulse of $\lambda = 632$ nm and (b) a two-dimensional magnetic lattice with $\alpha_s = \alpha_h = 3.5$ μm, $\tau = 2$ μm, and $\lambda = 532$ nm.

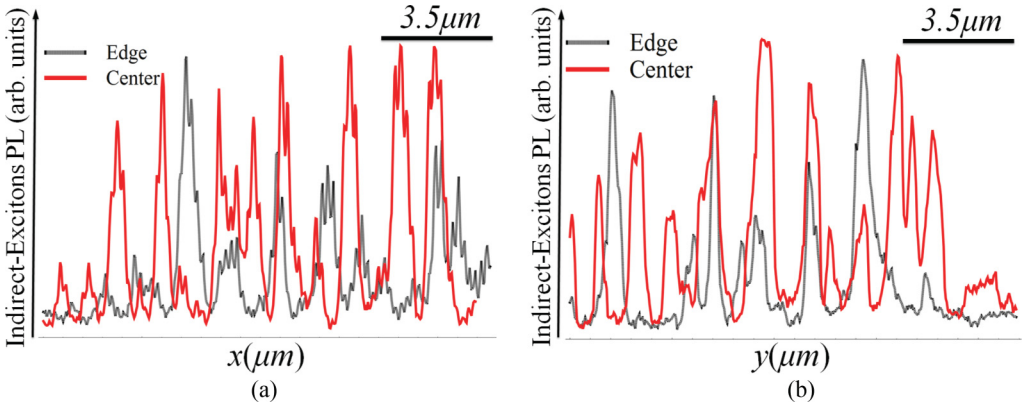

FIG. 5. (Color online) (a),(b) Comparison of the number of trapped indirect excitons at the center and at the edge of a two-dimensional magnetic lattice along the x and the y axis, respectively. Due to the asymmetrical distribution of the magnetic single traps (sites) a large number of trapped indirect excitons is found to concentrate at the center sites of the lattice. Experimental parameters as in Fig. 3(d).

sample. The existence of the fabricated patterns distributes the magnetic field accordingly as described above. In the case of the two-dimensional magnetic lattice, 3×3 blocks of 9×9 square holes are fabricated as shown in Fig. 4(b).

Indirect excitons are known to have long lifetimes, orders of magnitude longer than direct excitons, and can propagate farther in space at a bound e-h state before being recombined.[22] Here, the indirect excitons are formed in and drift to the vicinity of each single magnetic trap via distinct photoassisted capture along with the injection of electrons and holes. As shown in Fig. 5 the asymmetrical distribution of the magnetic single traps[15] can also be detected by scanning the number of trapped indirect excitons per site at the center and at the edge of the two-dimensional magnetic lattice, revealing the signature of the magnetic confinement of the indirect excitons.

The gate voltage V_G controls the electric field between the separated electron and hole layers. Increasing V_G results in enhancement of the indirect exciton emitted photoluminescence (PL) intensity with respect to the e-h density.[23] Figures 4(a) and 4(b) show enhanced photoluminescence as the gate voltage V_G increases for the cases of two- and one-dimensional magnetic lattices, respectively. The experimental result shown in Fig. 4(a) is for a one-dimensional magnetic lattice structure excited separately by using a NeHe laser ($\lambda = 632$ nm) while the result shown in Fig. 4(b) is for a two-dimensional magnetic lattice excited using a Nd:YAG laser ($\lambda = 532$ nm).

As observed in Fig. 6, the density of the trapped clouds increases as the power of the excitation laser increases merely because of the environmental fluctuations, and the indirect exciton scattering is smoothed out due to the magnetic confinement, which localizes the trapped particles in a space of limited degrees of freedom. Figure 6 shows the enhanced concentration of the indirect excitons as the laser power increases at $\lambda = 532$ nm. The drift of the indirect excitons towards the single traps could be mainly due to the interaction of these particles with the magnetic field where they are attracted towards space points of minimum magnetic values. At a relatively far distance from the excitation laser spot the concentration of the trapped particles declines, as illustrated in Fig. 6, where the excitation laser is set at the left bottom corner of the two-dimensional structure. We noticed that increasing the power of the excitation laser increases the number of magnetically trapped particles at far distances. The increased number of particles in each single magnetic field local minimum (single trap), even though the excitation pulse is set relatively far away, may indicate the drift of the indirect excitons towards the periodically distributed minimum values of the magnetic field.

In this type of magnetic trapping, external magnetic bias fields are often used to increase the magnetic trapping field's minimum value away from zero to prevent a Majorana spin-flip process of trapped particles.[15] The Majorana spin-flip process is avoided here because the zero point of the magnetic field

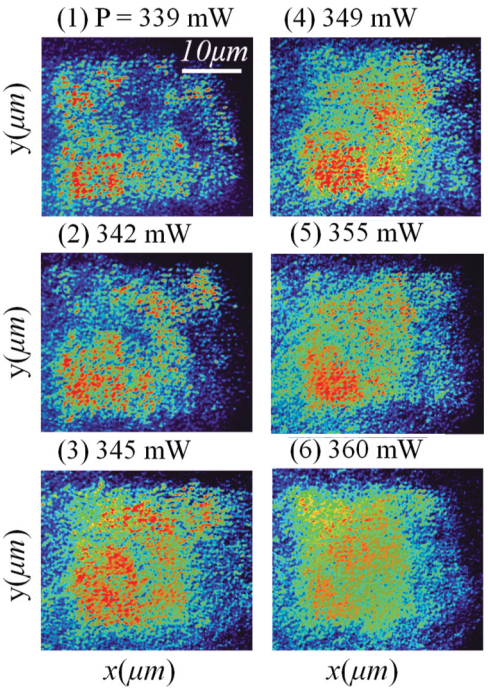

FIG. 6. (Color online) Nd:YAG pump laser with wavelength $\lambda = 532$ nm is used to examine the effect of varying the excitation power P_{laser} on the concentration of the trapped indirect excitons for the case of a two-dimensional magnetic lattice.

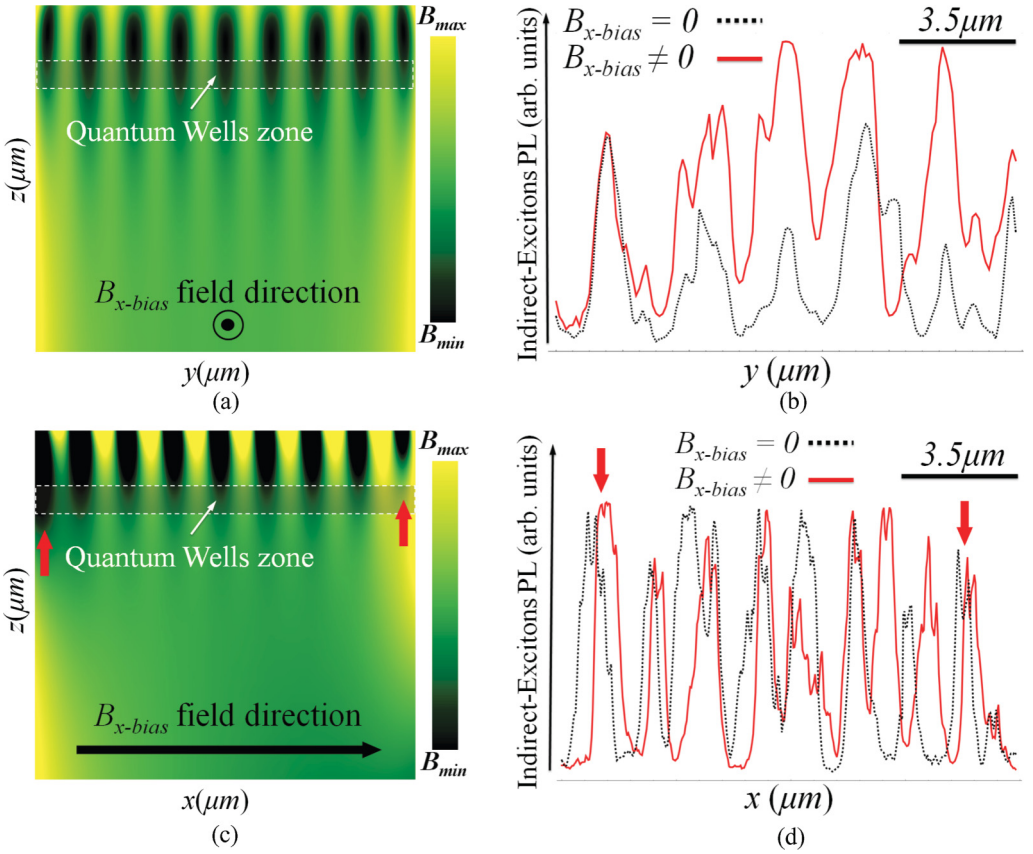

FIG. 7. (Color online) (a),(c) Simulation results of applying an external magnetic bias field along the x axis for a two-dimensional magnetic lattice with simulation parameters $\alpha_h = \alpha_s = 3.5\ \mu$m, $n = 9$ sites, $\tau = 2\ \mu$m, and magnetic bias field $B_{x\ \text{bias}} = 75$ G. (b) Experimental results for measured PL intensity along the y axis showing the increased number of trapped indirect excitons between the sites. (d) Shifts in the center of each single trap along the x axis due to the application of $B_{x\ \text{bias}}$. The red arrows in (c) and (d) indicate the change in the number of trapped indirect excitons per site due to the application of $B_{x\ \text{bias}}$.

local minima is located away from the formation plane of the indirect excitons. However, the effect of the external magnetic bias field can be used as a clear signature to identify the magnetic trapping of the indirect excitons as we show in Fig. 7 for the case of two-dimensional magnetic lattices. Moreover, applying external magnetic bias fields along the x, y, and/or z trapping axes allows to control the sites location and the number of the trapped particles in a magnetic lattice. Such bias fields can be used to induce tunneling of trapped particles between sites for a lattice with sufficiently small dimensions. They also allow to evaporatively cool down the trapped individual clouds.

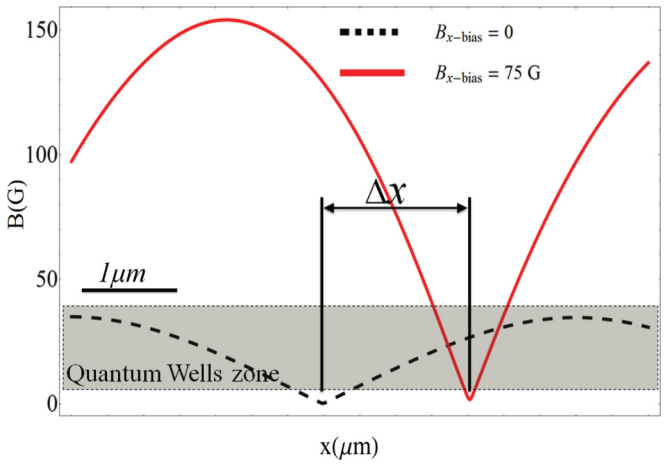

FIG. 8. (Color online) Simulation results showing the displacement Δx of each magnetic site across the formation plane of the indirect excitons due to the application of $B_{x\ \text{bias}}$. Simulation parameters are $\alpha_h = \alpha_s = 3.5\ \mu$m, $n = 9$ sites, and $\tau = 2\ \mu$m.

The simulation results in Figs. 7(a), 7(c), and 8 show the effect of applying an external magnetic bias field along the x axis for a two-dimensional magnetic lattice of dimensions $\alpha_h = \alpha_s = 3.5\ \mu$m, $n = 9$ sites, and $\tau = 2\ \mu$m, in which case the external bias fields modulate the location and the magnetic minimum value (magnetic bottom) of each single trap. While the modulating field increases the magnetic bottom and deforms the distribution of the traps along the applied field direction (x axis) it causes no change in the asymmetrical distribution of the traps along the direction (y axis) perpendicular to the applied magnetic field.[15]

Such a scenario is observed in our approach of magnetic confinement; an external magnetic bias field of $B_{\text{bias}} \approx 75$ G is applied along the x axis, resulting in increased numbers of trapped indirect excitons between the sites along the y direction without deforming the asymmetrical distribution of the sites along that axis, as shown in Fig. 7(b). Meanwhile,

along the x axis a slight change in the shape of the magnetic lattice (i.e., disappearance of the asymmetrical distribution of the sites[9,10,15]) is observed due to the application of the external modulating magnetic field. As shown in Fig. 7(d), the external modulating magnetic bias field causes a shift of the center of each individual site along the applied field direction (the x axis). The bias field also affects the number of trapped indirect excitons per site; the number of particles decreases away from the external field source as the magnetic bottom of each site changes. This change is indicated as red arrows in Fig. 7(d).

To conclude, we observed magnetic trapping for indirect excitons in one- and two-dimensional magnetic lattices. Modulating external magnetic bias fields along the confinement direction may cause sufficiently cooled individual clouds of trapped indirect excitons to tunnel between sites. This approach is a suitable candidate for simulating condensed-matter systems and processing quantum information.

The authors acknowledge that this work was supported by the Creative Research Initiative Program (Grant No. 2011-0000433) of the Korean Ministry of Education, Science and Technology via the National Research Foundation. We also thank Australian National University and Edith Cowan University in Western Australia for their help in fabricating the sample.

[1] S. Zimmermann, G. Schedelbeck, A. Govorov, A. Wixforth, J. Kotthaus, M. Bichler, W.Wegscheider, and G. Abstreiter, Appl. Phys. Lett. **73**, 154 (1998).
[2] A. Hammack, N. Gippius, S. Yang, G. Andreev, L. Butov, M. Hanson, and A. Gossard, J. Appl. Phys. **99**, 066104 (2006).
[3] M. Remeika, J. C. Graves, A. T. Hammack, A. D. Meyertholen, M. M. Fogler, L. V. Butov, M. Hanson, and A. C. Gossard, Phys. Rev. Lett. **102**, 186803 (2009).
[4] A. Winbow, J. Leonard, M. Remeika, Y. Kuznetsova, A. High, A. Hammack, L. Butov, J. Wilkes, A. Guenther, A. Ivanov *et al.*, Phys. Rev. Lett. **106**, 196806 (2011).
[5] R. Rapaport, G. Chen, S. Simon, O. Mitrofanov, L. Pfeiffer, and P. M. Platzman, Phys. Rev. B **72**, 075428 (2005).
[6] G. Chen, R. Rapaport, L. N. Pffeifer, K. West, P. M. Platzman, S. Simon, Z. Vörös, and D. Snoke, Phys. Rev. B **74**, 045309 (2006).
[7] A. A. High, A. K. Thomas, G. Grosso, M. Remeika, A. T. Hammack, A. D. Meyertholen, M. M. Fogler, L. V. Butov, M. Hanson, and A. C. Gossard, Phys. Rev. Lett. **103**, 087403 (2009).
[8] L. V. Butov, C. W. Lai, A. L. Ivanov, A. C. Gossard, and D. S. Chemla, Nature (London) **417**, 47 (2002).
[9] M. Remeika, M. Fogler, L. Butov, M. Hanson, and A. Gossard, Appl. Phys. Lett. **100**, 061103 (2012).
[10] Y. Kuznetsova, A. High, and L. Butov, Appl. Phys. Lett. **97**, 201106 (2010).
[11] J. A. K. Freire, A. Matulis, F. M. Peeters, V. N. Freire, and G. A. Farias, Phys. Rev. B **61**, 2895 (2000).
[12] J. A. K. Freire, F. M. Peeters, A. Matulis, V. N. Freire, and G. A. Farias, Phys. Rev. B **62**, 7316 (2000).
[13] Z. G. Koinov, G. Collins, and M. Mirassou, Phys. Status Solidi B **243**, 4046 (2006).
[14] A. Abdelrahman, H. Kang, S. Y. Yim, M. Vasiliev, K. Alameh, and Y. T. Lee, J. Appl. Phys. **110**, 013710 (2010).
[15] A. Abdelrahman, M. Vasiliev, K. Alameh, and P. Hannaford, Phys. Rev. A **82**, 012320 (2010).
[16] J. A. K. Freire, F. M. Peeters, A. Matulis, V. N. Freire, and G. A. Farias, Phys. Rev. B **62**, 7316 (2000).
[17] J. Levy, V. Nikitin, J. M. Kikkawa, A. Cohen, N. Samarth, R. Garcia, and D. D. Awschalom, Phys. Rev. Lett. **76**, 1948 (1996).
[18] S. Whitlock, R. Gerritsma, T. Fernholz, and R. Spreeuw, New J. Phys. **11**, 023021 (2009).
[19] J. Feldmann, G. Peter, E. O. Göbel, P. Dawson, K. Moore, C. Foxon, and R. J. Elliott, Phys. Rev. Lett. **59**, 2337 (1987).
[20] S. Ghanbari, T. D. Kieu, A. Sidorov, and P. Hannaford, J. Phys. B **39**, 847 (2006).
[21] P. C. Wo, P. R. Munroe, M. Vasiliev, Z. H. Xie, K. Alameh, and V. Kotov, Opt. Mater. **32**, 315 (2009).
[22] A. Gärtner, A. Holleithner, J. Kotthaus, and D. Schul, Appl. Phys. Lett. **89**, 052108 (2006).
[23] V. Negoita, D. W. Snoke, and K. Eberle, Phys. Rev. B **61**, 2779 (2000).